



# Richardson extrapolation with SubGrid to reduce the field discretization error in computational fluid dynamics

C. A. R. de Carvalho Jr<sup>1</sup> · C. H. Marchi<sup>1</sup> · C. D. Santiago<sup>2</sup>

Received: 14 July 2025 / Accepted: 3 February 2026  
© The Author(s) 2026

## Abstract

This work investigates the application of Richardson Extrapolation (RE) and its variants, including the Repeated Richardson Extrapolation (RRE) and the Completed Richardson Extrapolation (CRE) with polynomial interpolation, to improve the accuracy of numerical solutions in Computational Fluid Dynamics (CFD) problems. The study focuses on reducing the field discretization error through the coupling of extrapolation techniques with SubGrid strategies, an aspect rarely explored in the literature. The proposed method, referred to as Richardson Extrapolation with SubGrid (RES), is evaluated and compared with the CRE-I, FRE, and RRES approaches using the Finite Difference Method (FDM) with the second-order central difference scheme (CDS-2). The 2D Poisson, 1D and 2D Burgers, and 2D Navier–Stokes equations are solved on uniform and non-uniform grids, with known analytical solutions used to assess the discretization error. The results show that RE and RRE with SubGrid effectively reduce the discretization error, allowing for accuracy orders of 12 and 34. The RES method exhibits superior performance due to the local transfer of extrapolated information between coincident grid points, which suppresses truncation errors before they propagate. These methods are robust, simple to implement, and constitute efficient post-processing tools for improving numerical accuracy in CFD simulations.

**Keywords** Richardson extrapolation · SubGrid · CFD · Interpolation · CRE · FRE · RRE

## 1 Introduction

Richardson Extrapolation (RE) [1, 2] is a method used in the post-processing phase to reduce and estimate the discretization error of numerical solutions of differential equations. As a consequence, there is a reduction in CPU time and

computational memory required to solve a problem with a given error level [3]. The basic RE method requires knowing the numerical solution of the variable of interest on two computational grids with different numbers of nodes in the post-processing phase.

RE is an old method [1], however, with technological advances in computing, especially the development of more powerful processors and memory, several scientific studies have been published emphasizing lower discretization errors and more accurate solutions [4, 5]. The successive application of RE gives rise to a new method called Repeated Richardson Extrapolation (RRE) [2]. In this method, each application of RE represents another level of extrapolation, and it is necessary to have three or more numerical solutions available with different numbers of nodes [6, 7]. Erturk et al. [7] applied RRE with two levels of extrapolation to the numerical solution of the Navier–Stokes equations using the streamfunction-vorticity formulation in the classical lid-driven cavity problem for various Reynolds numbers. They achieved sixth-order of accuracy based on a second-order approach. Marchi et al. [3] used RRE in a 2D heat transfer problem to obtain highly accurate numerical

---

C. A.R. de Carvalho Jr and C. H. Marchi contributed equally to this work.

---

Technical Editor: Daniel Onofre de Almeida Cruz

---

✉ C. D. Santiago  
cosmo@utfpr.edu.br  
C. A. R. de Carvalho Jr  
carloscarvalhoj@gmail.com  
C. H. Marchi  
chmcf@gmail.com

<sup>1</sup> Department of Mechanical Engineering, Federal University of Paraná (UFPR), Curitiba, Paraná, Brazil

<sup>2</sup> Department of Matematics, Federal University of Technology - Paraná (UTFPR), Apucarana, Paraná, Brazil

solutions. They demonstrated that RRE is extremely effective in reducing the discretization error of both primary and secondary variables, regardless of the number of numerical approximations employed, in addition to other important findings that highlight the value of the RRE method. Marchi et al. [8] introduced a new methodology in which polynomial interpolation was applied to numerical solutions of local variables obtained at different grid points, followed by RRE. Four CFD problems were used to test the proposed procedure, including the 2D Navier–Stokes equations. Among their conclusions, they pointed out that RRE is more suitable for global variables or local variables with a fixed location that coincides with a nodal point in each considered grid. They also demonstrated that the discretization error was significantly reduced, the order of accuracy was increased, and the computational effort was required to obtain the solution at a given numerical error level. In Silva et al. [9], the RRE method was applied to local and global variables obtained using the Smoothed Particle Hydrodynamics (SPH) method. They showed that RRE is robust in achieving up to sixteenth-order of accuracy in meshless discretization for the spatial domain.

Other methods used to reduce discretization error based on Richardson extrapolation can also be found in the literature. Considered an extended version of RE for solution fields, the Completed Richardson Extrapolation (CRE) was developed by Roache and Knupp [10]. In CRE, a Richardson extrapolation is applied to solutions obtained on two grids. They used the one-dimensional Poisson equation with different source terms, the Advection-Diffusion equation with different Peclet numbers, and the two-dimensional Poisson equation in a unit domain. They concluded that the method produces a fourth-order accurate solution on a SubGrid, combining second-order solutions on the fine grid and the SubGrid, and is “complete” in the sense that a higher-order accurate solution is obtained at all nodes of the fine grid. In [11], a procedure based on CRE was proposed for grids with possibly non-coincident nodes,

which are frequently used in compressible flows. The developed method called Completed Repeated RE (CRRE), was tested on numerical solutions of one-dimensional and quasi-one-dimensional Euler equations with steady-state solutions. An excellent performance of CRRE was observed in the test problems, where the error was reduced by seven orders of magnitude.

A new method, Full Richardson Extrapolation (FRE), was developed by Marchi et al. [12], combining the features of CRE and RRE. The method was used in solution fields for one-dimensional and two-dimensional problems in Computational Fluid Dynamics (CFD), including the 2D Burgers equations with  $Re=1$ . They observed that both FRE and CRE methods produce fourth-order of accuracy in

reducing the discretization error across all tested models: Poisson equations, 1D advection-diffusion, 2D Laplace, and 2D Burgers equations in the velocity variable,  $u$ .

In [13], the development of extrapolation processes in numerical analysis is emphasized, mainly focusing on those based on polynomial or rational functions. An extensive bibliographic review was conducted, presenting the most important contributions and making interconnections between works in different areas. A study on the cost of extrapolation methods was conducted by Silvana et al. [14]. They used the explicit midpoint rule and showed that the cost of reducing the error is polynomial in the number of precision digits for numerical sequences with at most an arithmetic growth, and exponential for numerical sequences with at least a geometric growth. Convergence analyses for a nearly singularly perturbed linear problem, with an integral boundary condition and adaptive grid, can be found in [15].

More recently, several studies have demonstrated that Richardson extrapolation and its variants remain an active research topic. In [16], it was demonstrated that Completed Richardson Extrapolation (CRE), when combined with geometric multigrid, can yield higher-order accurate solutions for the Poisson equation without modifying the underlying discretization stencil. Fekete et al. [17] established theoretical results demonstrating that repeated Richardson extrapolation (RRE) can systematically increase the convergence order of linear multistep methods, formally reinforcing the effectiveness of RRE as a tool for improving accuracy order. In a broader context [18], introduced a generalized form of extrapolation, called Layerwise Richardson Extrapolation (LRE), capable of handling multi-parameter error structures in quantum systems, highlighting the modern trend of extending Richardson-based methods to more flexible and localized error models. These recent contributions confirm the growing interest in advanced extrapolation strategies and support the motivation for exploring RE with SubGrid approaches.

Unlike adaptive grid refinement techniques that combine SubGrid resolution with error estimators, the RES and RRES methods used in this work operate strictly as post-processing procedures and do not modify the solver or the grid. This independence from the numerical discretization and the absence of refinement criteria define the main novelty of the present approach and distinguish it from state-of-the-art SubGrid-based error-reduction methods.

The methods mentioned above generally provide good results when applied according to their characteristics. In addition to fulfilling their purpose of reducing

discretization error, they also reduce computational cost, which is essential in engineering design scaling. In this context, it is important to emphasize the constant need to

improve numerical solutions. The methods based on Richardson extrapolation fit into this context as excellent auxiliary tools, with their enhancement being crucial for use in various types of problems that arise in CFD.

The focus of the present research is to contribute to the literature by adding SubGrid and polynomial interpolation to Richardson extrapolation. Therefore, the aim is to continue improving RE by using different types of grids to obtain more accurate solutions across the entire solution field of some mathematical models.

In CFD, it is common to use non-uniform grids in numerical simulations due to their greater versatility in adapting to physical phenomena. In this work, three types of structured grids are adopted: (a) uniform grids, (b) non-uniform grids, and (c) directionally non-uniform grids, and their use aims to evaluate the performance of the extrapolation methods under distinct discretization scenarios, which is a key aspect of the present study’s objective, since the behavior and effectiveness of RE-based techniques depend on the local mesh distribution and error structure.

The following sections are organized as follows: Sect. 2 defines the mathematical and numerical models; Sect. 3 provides a brief overview of the methods’ design and methodology; Sect. 4 presents and discusses the post-processing results; and Sect. 5 provides the conclusion.

## 2 Mathematical and numerical models

As known in the literature, a common procedure to obtain numerical solutions for engineering problems is to divide the real domain into a finite number of points or control volumes, usually referred to as the computational grid [19], which is used to discretely represent the real domain of the mathematical model. The Finite Volume Method (FVM) [19] and the Finite Difference Method (FDM) [20] are frequently used to approximate the derivatives that arise in the governing equations. In the present work, FDM is adopted in three types of structured grids, Fig. 1. In the uniform grid, Fig. 1a, the distances between two consecutive points are equal. In the non-uniform grid, Fig. 1b, the distances between two consecutive points are not necessarily equal. If the grid is uniform in direction, Fig. 1c, the distances

between two consecutive points are equal only in each spatial direction,  $x$  or  $y$ .

In grids, as illustrated in Fig. 1, Richardson Extrapolation will be applied to the numerical solutions of four common mathematical models in CFD problems. All cases are considered in a unit domain, where  $(x, y) \in [0, 1]$  are the spatial coordinates. The choice of models with known analytical solutions is justified by the need to measure the numerical error to assess the performance of the methods. The boundary conditions are applied based on the corresponding analytical solution. The models are described below.

### 1. Nonlinear 1D Burgers equation

$$vRe \frac{dv}{dx} = \frac{d^2v}{dx^2} + \frac{Re^2 e^{xRe} (e^{xRe} - e^{Re})}{(e^{Re} - 1)^2}. \tag{1}$$

The analytical solution of Eq. (1) is given by

$$v(x) = \frac{e^{xRe} - 1}{e^{Re} - 1}, \tag{2}$$

where the field variable  $v$  is the flow velocity,  $Re=1$  is the Reynolds number.

### 2. 2D Poisson equation

$$\frac{\partial^2 T}{\partial x^2} + \frac{\partial^2 T}{\partial y^2} = e^y (1 - \frac{\pi^2}{4}) \sin(\frac{\pi}{2} x). \tag{3}$$

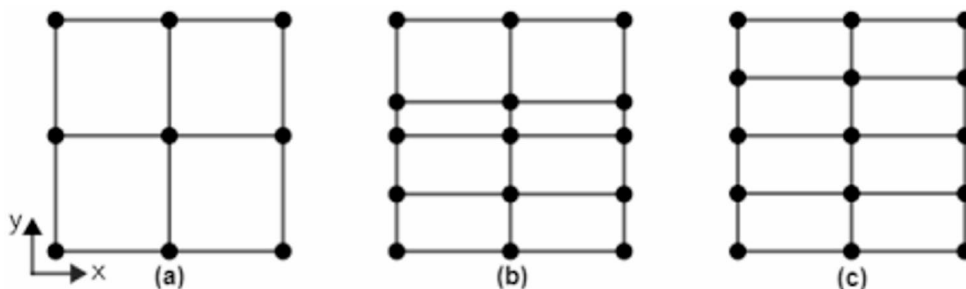
The analytical solution of Eq. (3) is given by

$$T(x, y) = e^y \sin(\frac{\pi}{2} x) \tag{4}$$

where the field variable  $T$  is a physical quantity.

### 3. Nonlinear 2D Burgers equations

Fig. 1 Two-dimensional grids in several configurations



$$\begin{aligned}
 u \frac{\partial u}{\partial x} + v \frac{\partial u}{\partial y} &= \frac{1}{Re} \left( \frac{\partial^2 u}{\partial x^2} + \frac{\partial^2 u}{\partial y^2} \right) - \frac{\partial p}{\partial x}, \\
 u \frac{\partial v}{\partial x} + v \frac{\partial v}{\partial y} &= \frac{1}{Re} \left( \frac{\partial^2 v}{\partial x^2} + \frac{\partial^2 v}{\partial y^2} \right) - \frac{\partial p}{\partial y} + S,
 \end{aligned}
 \tag{5}$$

where  $u$  and  $v$  are the velocities in the directions of the  $x$  and  $y$  axes, respectively,  $p$  is the pressure,  $Re$  is the Reynolds number, and  $S$  is the additional source term introduced due to the manufactured solution [21]. The analytical solution of the system given by Eq. (5) is, Shih et al. [22],

$$\begin{aligned}
 u(x, y) &= 8(x^4 - 2x^3 + x^2)(4y^3 - 2y), \\
 v(x, y) &= -8(4x^3 - 6x^2 + 2x)(y^4 - y^2),
 \end{aligned}
 \tag{6}$$

#### 4. Navier-Stokes equations - streamfunction–vorticity formulation

The two-dimensional Navier–Stokes equations for an incompressible viscous flow, written in terms of the vorticity transport equation and streamfunction equation ( $\psi$ ,  $\omega$ ), are given by [23],

$$\begin{aligned}
 \frac{\partial \psi}{\partial x} + \frac{\partial \psi}{\partial y} &= -\omega, \\
 \frac{\partial \omega}{\partial x} + \frac{\partial \omega}{\partial y} &= Re \left( \frac{\partial \psi}{\partial y} \frac{\partial \omega}{\partial x} - \frac{\partial \psi}{\partial x} \frac{\partial \omega}{\partial y} \right) + S,
 \end{aligned}
 \tag{7}$$

where  $\psi$  is the streamfunction and  $Re$  is the Reynolds number,  $S$  is a term that arises due to the manufactured solution. The vorticity equation is given by

$$\omega = \frac{\partial v}{\partial x} - \frac{\partial u}{\partial y}.
 \tag{8}$$

The Eq. (7) are Poisson-like equations and are coupled by the variables  $\psi$  and  $\omega$ . The velocity components are defined in terms of streamfunction as follows

$$u = \frac{\partial \psi}{\partial y}, \quad v = -\frac{\partial \psi}{\partial x}.
 \tag{9}$$

The analytical solution of the system given by Eq. (7) is

Grid	scheme									
$g = 1$	• <sub>1</sub>									• <sub>2</sub>
$g = 2$	• <sub>1</sub>			• <sub>2</sub>						• <sub>3</sub>
$g = 3$	• <sub>1</sub>		• <sub>2</sub>		• <sub>3</sub>		• <sub>4</sub>			• <sub>5</sub>
$g = 4$	• <sub>1</sub>	• <sub>2</sub>	• <sub>3</sub>	• <sub>4</sub>	• <sub>5</sub>	• <sub>6</sub>	• <sub>7</sub>	• <sub>8</sub>	• <sub>9</sub>	

Fig. 2 Location of extrapolation points in one-dimensional grids with finite differences

$$\begin{aligned}
 \psi(x, y) &= 8(x^4 - 2x^3 + x^2)(y^4 - y^2), \\
 \omega(x, y) &= -8(12x^2 - 12x + 2)(y^4 - y^2) - 8(x^4 - 2x^3 + x^2)(12y^2 - 2).
 \end{aligned}
 \tag{10}$$

The analytical solution of the velocities, Eq. (9), is given by Eq. (6). The values of  $\psi$  and  $\omega$  at the boundaries are obtained from Eqs. (10), and the velocities at the boundaries are obtained from Eq. (6). All derivatives are approximated using the Finite Difference Method with the second-order CDS-2 (Central Difference Scheme). In Eq. (1), uniform and non-uniform grids are used, and the resulting system of equations is solved with the iterative TDMA solver [24]. In Eq. (3), uniform and directionally non-uniform grids are used. The system of equations resulting from Eq. (5) is solved with the MSI (Modified Strongly Implicit) solver [25]. The Gauss-Seidel solver [26] is used for the system of equations arising from the 2D Poisson and the Navier-Stokes equations, Eq. (7). The geometric multigrid method with V-cycle [5, 23] is used in the two-dimensional models to accelerate the convergence of the iterative methods. The velocities, Eq. (9), are approximated with second-order of accuracy (CDS-2) on the finest grid of each V-cycle of the multigrid method during the iterative process.

Regardless of the grid type, whether uniform or non-uniform, a uniform refinement with a ratio of  $r=2$  is used. In this case, the orders of accuracy of the method are the same, which is important for post-analysis. The parameter  $r=2$  represents the refinement factor between two consecutive grids, meaning that the finer grid contains twice as many intervals (and therefore nodes) in each spatial direction compared to the immediately coarser grid. For the non-uniform grids considered in this work, the refinement ratio  $r=2$  is maintained by doubling the number of intervals in each coordinate direction while preserving the same stretching distribution. Thus, the non-uniform spacing function is kept identical across refinement levels, and all local steps are scaled by 1/2. This guarantees that corresponding spacings satisfy  $h_{\text{coarse}} = 2h_{\text{fine}}$ , ensuring the validity of Richardson extrapolation even under directional non-uniformity.

Due to the use of manufactured solutions, the simulations associated with Eqs. (5) and (7) are carried out with a unit Reynolds number [27]. To eliminate iteration errors, in all simulations, the solver was run until the machine rounding error was reached with quadruple precision (Real\*16).

### 3 Methods and methodology

In this section the extrapolation methods used in the numerical simulations are presented. To better illustrate them, consider four one-dimensional grids, as shown in Fig. 2. The coarser grid,  $g=1$ , has two nodes; the others are obtained through uniform refinement with a ratio of two.

In Fig. 2, the existence of coincident points can be observed. The subsequent finer grids contain the points of the coarser grids, i.e., the grid  $g=4$  contains the points of grids  $g=3$ ,  $g=2$ , and  $g=1$ . This concept is important for the following steps of the methodology in the application of post-processing methods, whose goal is to simultaneously reduce the numerical error of all points in the chosen grid. In the following sections, the methods used with a focus on this objective are presented.

### 3.1 SubGrid variations with RE and RRE

Richardson Extrapolation (RE) is built from the Taylor Series using numerical approximation with a spacing of  $h$  between two consecutive nodes. At least two numerical solutions  $\phi(h)$  and  $\phi(rh)$  are required, which correspond to the values obtained in the discretized domains  $\Omega^h$  (fine grid) and  $\Omega^{rh}$  (coarse grid), where  $rh > h$ . The relationship between the two grids is given by the refinement ratio  $r$ , preferably uniform. The RE can be written as [28],

$$\Phi = \phi_\infty + c_0 h^{p_0} + c_1 h^{p_1} + c_2 h^{p_2} + \varepsilon_T(h^{p_3}), \tag{11}$$

in which the coefficients  $c_i$  are constants, not necessarily positive. The exponents  $p_0, p_1, p_2, \dots$  of  $h$ , of the non-zero terms in Eq. (11), represent the true orders of the discretization error [10], monotonically increasing,  $1 \leq p_0 \leq p_1 \leq p_2 < \dots$ . The smallest exponent of  $h$  in Eq. (11) is called the asymptotic order. With grid refinement, the first term of  $h$  begins to dominate over the others, and the numerical solution can be written as [29],

$$\phi = \phi_\infty + c_1 h^{p_v}, \quad p_v = 1, 2, 3, \dots, \tag{12}$$

in which  $\phi_\infty$  represents an approximation to the exact analytical solution or the extrapolated solution, given by

$$\phi_\infty(h) = \phi(h) + \frac{\phi(h) - \phi(rh)}{r^{p_v} - 1}. \tag{13}$$

When the order of accuracy of the numerical approximation of the derivatives is second order (CDS-2), the true orders of the error are  $p_v = 2, 4, 6, \dots$ .

The Repeated Richardson Extrapolation (RRE) [9, 10] is obtained by applying Eq. (13) recursively on  $G$  distinct grids  $\Omega^{h^1}, \Omega^{h^2}, \Omega^{h^3}, \Omega^{h^2}, \dots, \Omega^{h^g}, \dots, \Omega^{h^G}$ , generated with a refinement ratio  $r = h^{s-1}/h^s, g = 2, \dots, G$ , where the equation is obtained

$$\phi_{g,m} = \phi_{g,m-1} + \frac{\phi_{g,m-1} - \phi_{g-1,m-1}}{r^{p_{m-1}} - 1}, \quad g = 2, \dots, G; \quad m = 1, \dots, g-1 \tag{14}$$

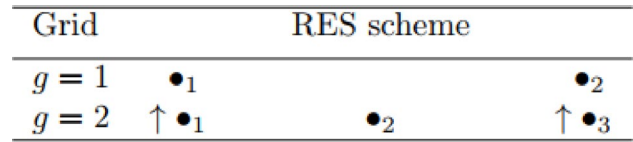


Fig. 3 Schematic representation of the RES method,  $g=1$

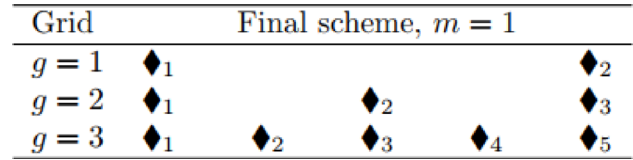


Fig. 4 Final scheme with RES for a single extrapolation,  $m=1$

in which  $m$  indicates the extrapolation level and  $g$  the grid number. The variables  $\phi_{1,0}, \phi_{2,0}, \phi_{3,0}, \dots, \phi_{G,0}$  represent the numerical solutions  $\phi_1, \phi_2, \phi_3, \dots, \phi_G$  obtained on the grids  $\Omega^{h^1}, \Omega^{h^2}, \Omega^{h^3}, \Omega^{h^2}, \dots, \Omega^{h^g}, \dots, \Omega^{h^G}$ , respectively, without extrapolation, i.e.,  $m=0$ .

A methodology proposed in this work can be understood with the application of the grid  $g=2$  of Fig. 2, where only the coincident points are used. The points  $\bullet_1$  e  $\bullet_3$ , Fig. 3 for  $g=2$  are injected ( $\uparrow$ ) into the grid  $g=1$  using RE, replacing their solutions with their extrapolated versions, whose accuracy is theoretically higher. This concept will be denoted as SubGrid, that is, Richardson Extrapolation with SubGrid (RES).

The process is repeated for grid  $g=2$ , using  $g=3$  as support, then for grid  $g=3$ , using  $g=4$ . Thus, three grids can be obtained with an extrapolation through RES, as shown in Fig. 4. The extrapolated grid point is denoted as  $\blacklozenge_i$ . It is observed that, with the continuation of the process, it is possible to obtain new extrapolated grids, similar to RRE, in which the finest grid is always discarded.

An alternative approach to using SubGrid consists of the direct application of RRE, optimizing one grid at a time. In this process, when selecting a grid, its predecessors are automatically discarded. For example, considering Fig. 2, choosing grid  $g=2$  eliminates grid  $g=1$ . Similarly, selecting grid  $g=3$  discards both grids  $g=1$  and  $g=2$ . Subsequently, in the following grids, the nodes coinciding with the chosen grid are isolated, and RRE is applied only to these points.

Figure 5 illustrates the final scheme of this approach, using the example for  $g=1$ . In this scheme,  $\bullet_i(m)$  refers to the point at position  $i$  on the grid with  $m$  extrapolations (where  $m=0$  is the initial grid without extrapolations). The extrapolation used at each  $\bullet_i(m)$  is the first obtained for each point. In the illustrated case, it was possible to perform three extrapolations. This method is called RRE with SubGrid (RRES).

One way to optimize the finer grid with SubGrid, in the initial case with  $g=4$  or any other set of points  $\beta$  without

Grid	Final scheme, $g = 1$	
$g = 1$	$\bullet_1(0)$	$\bullet_2(0)$
$g = 2$	$\bullet_1(1)$	$\bullet_3(1)$
$g = 3$	$\bullet_1(2)$	$\bullet_5(2)$
$g = 4$	$\bullet_1(3)$	$\bullet_9(3)$

Fig. 5 Final scheme with RRES for the grid  $g=1$

Grid	Initial scheme									
$g = 1$	$\bullet_1$	$\times_1$	$\times_2$	$\times_3$	$\times_4$	$\times_5$	$\times_6$	$\times_7$	$\bullet_2$	
$g = 2$	$\bullet_1$	$\triangleright_1$	$\triangleright_2$	$\triangleright_3$	$\bullet_2$	$\triangleright_4$	$\triangleright_5$	$\triangleright_6$	$\bullet_3$	
$g = 3$	$\bullet_1$	$\nabla_1$	$\bullet_2$	$\nabla_2$	$\bullet_3$	$\nabla_3$	$\bullet_4$	$\nabla_4$	$\bullet_5$	
$g = 4$	$\bullet_1$	$\bullet_2$	$\bullet_3$	$\bullet_4$	$\bullet_5$	$\bullet_6$	$\bullet_7$	$\bullet_8$	$\bullet_9$	

Fig. 6 Initial scheme for RRES-I,  $g=4$

coincident points between grids, is through polynomial interpolation. Approximating functions with polynomials is one of the oldest ideas in numerical analysis and remains one of the most widely used techniques in the field [15]. This is because polynomials are easily computable, their integrals and derivatives are straightforward to obtain, and their roots can be determined, when possible, in a reasonably simple manner.

Consider  $\beta$  as the set of points of the  $g=4$  grid shown in Fig. 2. If any point is missing from the grid, interpolations are performed. For example, in the  $g=1$  grid from Fig. 6, the points  $x_i$  are obtained through interpolations using only the available points in the  $g=1$  grid. This procedure is repeated for the  $g=2$  and 3 grids to obtain  $\triangleright_i$  and  $\nabla_i$ , respectively. In the  $g=4$  grid no interpolation is necessary since  $\beta$  already represents its set of points. In the RRES-I procedure, the interpolation polynomials were chosen with degrees between 2 and 10. This range reflects the actual number of supporting points available in the grid hierarchy. To construct a polynomial of degree  $k$ , at least  $k+1$  distinct nodes are required in each direction, and the refined grids used in this work provide enough points to allow interpolation up to degree 10.

This is the initial step of RRES for  $\beta$  and the process continues with the repeated application of RE, as previously explained and illustrated in Fig. 7. We denote this method as Repeated Richardson Extrapolation with SubGrid and Interpolation (RRES-I).

Fig. 7 Final scheme for RRES-I with extrapolations and  $\beta$  being the finest grid,  $g=4$

Grid	Final scheme									
$g = 1$	$\bullet_1(0)$	$\times_1(0)$	$\times_2(0)$	$\times_3(0)$	$\times_4(0)$	$\times_5(0)$	$\times_6(0)$	$\times_7(0)$	$\bullet_2(0)$	
$g = 2$	$\bullet_1(1)$	$\triangleright_1(1)$	$\triangleright_2(1)$	$\triangleright_3(1)$	$\bullet_2(1)$	$\triangleright_4(1)$	$\triangleright_5(1)$	$\triangleright_6(1)$	$\bullet_3(1)$	
$g = 3$	$\bullet_1(2)$	$\nabla_1(2)$	$\bullet_2(2)$	$\nabla_2(2)$	$\bullet_3(2)$	$\nabla_3(2)$	$\bullet_4(2)$	$\nabla_4(2)$	$\bullet_5(2)$	
$g = 4$	$\bullet_1(3)$	$\bullet_2(3)$	$\bullet_3(3)$	$\bullet_4(3)$	$\bullet_5(3)$	$\bullet_6(3)$	$\bullet_7(3)$	$\bullet_8(3)$	$\bullet_9(3)$	



Fig. 8 Scheme for CRE on grid  $g=2$

### 3.2 Completed Richardson extrapolation with variations

The Completed Richardson Extrapolation (CRE) [10] is obtained when two grids, fine and coarse, are given, and it is possible to perform extrapolations at all points of the fine grid.

Let the grids  $g=1$  and  $g=2$  be as illustrated in Fig. 8. Then, it is only possible to apply RE to the points  $\bullet_1$  and  $\bullet_3$  of the  $g=2$ . In this case, unlike the SubGrid approach, it is the fine grid that receives ( $\downarrow$ ) the extrapolated points. For point  $\bullet_2$  information is injected ( $\rightarrow \searrow \swarrow \leftarrow$ ) from the points with coincident neighbors to complete the extrapolations on the  $g=2$  grid.

In [13], the authors showed that RE is only applicable to the odd nodes of the fine grid. To obtain accurate solutions at the even nodes, they transformed the fine grid into two SubGrids: the first one contains the odd points of the grid that have coincident points in the coarse grid, and the second one contains the even points.

The Completed Richardson Extrapolation can be summarized by the equation.

$$P \leftarrow P + C, \tag{15}$$

where  $P$  represents the set of points with numerical solutions from the grid that receives the original values plus the correction  $C$ , for each case of the SubGrid.

In this work, some variations of Eq. (15) are addressed, which will be illustrated with the one-dimensional case.

Let  $i=1,3,5,\dots, N_g$  nodes, with  $N_g$  odd, of grid  $g$ , for  $g=2, \dots, G$  grids, where  $g=1$  is the coarsest grid, and the others are obtained using uniform refinement with a ratio of two, adapted from [13], we have

$$\phi_{g,i}^m = \phi_{g,i}^{m-1} + C_{g,i}^m \tag{16}$$

where

$$C_{g,i}^m = \frac{\phi_{g,i}^{m-1} - \phi_{g-1,i}^{m-1}}{2^{p_0} - 1}, \tag{17}$$

$\phi$  represents the variable of interest,  $C$  the correction term,  $m$  the extrapolation level,  $g$  the grid number, and  $i$  the spatial position of the node in the grid. For the even nodes, we have

$$\phi_{g,i+1}^m = \phi_{g,i+1}^{m-1} + C_{g,i+1}^m, \tag{18}$$

with  $i=1,3,5,\dots,N_g - 2$ , in which.

1. Classical (CRE) adapted from [13]

$$C_{g,i+1}^m = \frac{C_{g,i}^m + C_{g,i+2}^m}{2}. \tag{19}$$

2. Interpolated (CRE-I): If possible, the corrections obtained at up to  $p+1$  coincident nodes around node  $i+1$  are interpolated, obtaining a polynomial  $\phi_p$  of maximum degree  $p$  and.

$$C_{g,i+1}^m = \varphi_p(x_{i+1}), \tag{20}$$

otherwise, the classical mode is adopted, Eq. (17).

3. Full Richardson Extrapolation (FRE), adapted from [11]

$$C_{g,i+1}^m = C_{g,i}^m + k(C_{g,i+2}^m - C_{g,i}^m), \tag{21}$$

in which  $k$  is the weighting factor given by the equation

$$k = \frac{\phi_{g,i+1}^{m-1} - \phi_{g,i}^{m-1}}{\phi_{g,i+2}^{m-1} - \phi_{g,i}^{m-1}}. \tag{22}$$

In the two-dimensional case, with the exception of CRE-I, the procedure is similar and can be seen in more detail in the referenced works. In CRE-I, interpolations can be performed in two ways: (a) in the traditional form using two-dimensional interpolations and (b) using one-dimensional interpolations by directions.

It is important to emphasize that for CRE-I, the interpolations must have orders equal to or higher than the orders of the numerical solutions, i.e.,  $p_0 \geq 2$ . It is recommended to establish a maximum interpolation order and use it whenever possible. In this work, interpolations with orders between 2 and 10 were employed. These levels can be achieved when the region of interest does not extend over the boundaries and the grid contains the necessary number

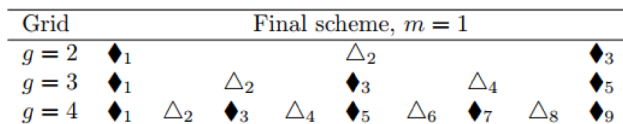


Fig. 9 Final scheme for an extrapolation using four grids,  $m=1$ , with CRE and variations

of points. For example, at least 11 points are required to obtain an interpolation of order 10 in linear interpolation. Interpolations as a way to improve extrapolations were also used by [10] and [14].

Figure 9 illustrates the final scheme for an extrapolation with CRE using four grids. The symbol  $\blacklozenge_i$  represents the points obtained with RE and  $L_i$  through some method presented earlier. It is possible to continue the extrapolations, but in this case, the coarsest grid is always discarded, unlike in RES.

The CRE was initially developed to perform only one extrapolation [13]. However, with appropriate modifications to the correction term  $C$ , it is possible to perform multiple extrapolations, i.e.,  $m > 1$ . Other ways of modifying  $C$  can be seen in [30, 31].

### 3.3 Variable of Interest and Grid Generation

In the present study, the variable of interest is the average of the discretization error magnitude,  $\ell_1$ -norm, given by

$$\ell_1(E(\phi)) = \frac{\sum_{i=1}^N |\Phi_i - \phi_i|}{N} \tag{23}$$

in which  $\phi$  is the numerical solution,  $\Phi$  is the exact analytical solution,  $N$  is the total number of internal points, and  $E$  is the discretization error given by  $E(\phi) = \Phi - \phi$  at each point  $i$  of the grid,  $i=1,2,3,\dots,N$ .

The accuracy of the numerical solutions is verified through a posteriori analyses based on the equivalent orders of accuracy, referred to as the effective order of the  $\ell_1$ -norm, given by

$$p_E = \frac{\log\left(\left|\frac{\Phi - \phi_1}{\Phi - \phi_2}\right|\right)}{\log(r)} \tag{24}$$

where  $\phi_1$  and  $\phi_2$  are the numerical solutions on the coarse and fine grids, respectively, and  $r=2$  is the refinement ratio. The expressions  $\Phi - \phi_1$  and  $\Phi - \phi_2$  refer to the  $\ell_1$ -norms calculated on the coarse and fine grids, respectively. Theoretically, the order of accuracy in CDS-2 is  $p_0=2$ , even on non-uniform grids. In the present work, the orders are multiples of 2.

On non-uniform grids, the coordinates of the points on the initial grid were selected randomly from the vectors  $h_x$  and  $h_y$ , which represent the distances between points in the  $x$  and  $y$  directions, as illustrated in Fig. 10.

The following grids were generated with a refinement ratio  $r=2$ . The initial vectors are shown below.

1. Burgers 1D

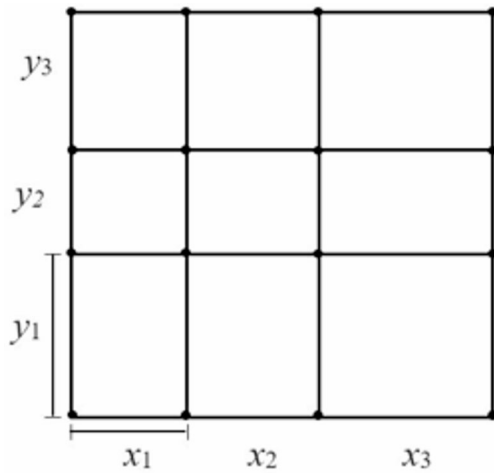


**Fig. 10** Example of a non-uniform grid illustrating  $x$  and  $y$  distances

$$\begin{aligned}
 h_x \approx & (6.85\text{E} - 08, 4.450\text{E} - 03, 6.16\text{E} - 02, \\
 & 1.16\text{E} - 01, 1.68\text{E} - 01, 1.46\text{E} - 01, 5.86\text{E} - 02, \\
 & 1.60\text{E} - 01, 1.39\text{E} - 01, 1.45\text{E} - 01)^T.
 \end{aligned} \tag{25}$$

2. Two-dimensional:  $5 \times 5$

$$\begin{aligned}
 h_x \approx & (3.75\text{E} - 07, 2.44\text{E} - 02, 3.37\text{E} - 01, 6.38\text{E} - 01)^T, \\
 h_y \approx & (3.16 - 01, 2.75\text{E} - 01, 1.10\text{E} - 01, 2.99\text{E} - 01)^T.
 \end{aligned} \tag{26}$$

3. Two-dimensional:  $7 \times 5$

$$\begin{aligned}
 h_x \approx & (1.38\text{E} - 07, 8.96\text{E} - 03, 1.24\text{E} - 01, 2.34\text{E} \\
 & -01, 3.38\text{E} - 01, 2.95\text{E} - 01)^T, \\
 h_y \approx & (1.16\text{E} - 01, 3.18\text{E} - 01, 2.76\text{E} - 01, 2.89\text{E} - 01)^T.
 \end{aligned} \tag{27}$$

### 4 Results and discussions

The computational codes were written in Fortran 90. The simulations were performed on a computer with a 64-bit Windows 10 operating system, 16 GB of RAM, and 2.4 GHz, with quadruple precision (Real\*16). It is important to note that all extrapolation-based techniques evaluated in this work (RES, RRES, CRE-I, RRES-I and FRE) operate strictly as post-processing procedures. Therefore, the additional computational cost associated with these methods is limited to local extrapolation/interpolation operations, which are negligible when compared with the dominant cost of solving the differential equations themselves. For this reason, no significant increase in CPU time or memory usage was observed in any of the simulations, and a dedicated performance table was deemed unnecessary.

Table 1 summarizes the mathematical models, variables of interest, and methods discussed. In the 2D Burgers and

**Table 1** Mathematical models and methods tested in present work

1D Burgers					
Uniform	RES	CRE-I	RRES	RRES-I	FRE
Non-uniform	RES	CRE-I		RRES-I	FRE
2D Burgers					
u velocity	RES	CRE-I	RRES		
v velocity	RES	CRE-I	RRES		
2D Poisson					
Uniform	RES	CRE-I			
Non-uniform by direction	RES	CRE-I			
Navier-Stokes					
$\psi$ streamfunction	RES	CRE-I			
$\omega$ vorticity	RES	CRE-I			
$u$ -velocity	RES	CRE-I			

2D Navier-Stokes equations, only uniform grids were used. All simulations were performed with different grid sizes, one of the requirements necessary for extrapolation. The solvers were run with sufficient iterations to reach machine rounding error, thus eliminating iteration error. The refinement ratio between the grids is  $r=2$ . The number of significant digits of the numerical solution without extrapolation is at least 32, and the theoretical order of accuracy is  $p_0=2$ , Eq. (11). The discretization error magnitude,  $\ell_1$ -norm, was calculated using Eq. (23), and the effective order  $p_E$  of the  $\ell_1$ -norm was calculated with Eq. (24), as described in Sect. 3.3. In the following subsections, the main results of the methods from Table 1 tested with the mathematical models described in Sect. 2 are highlighted.

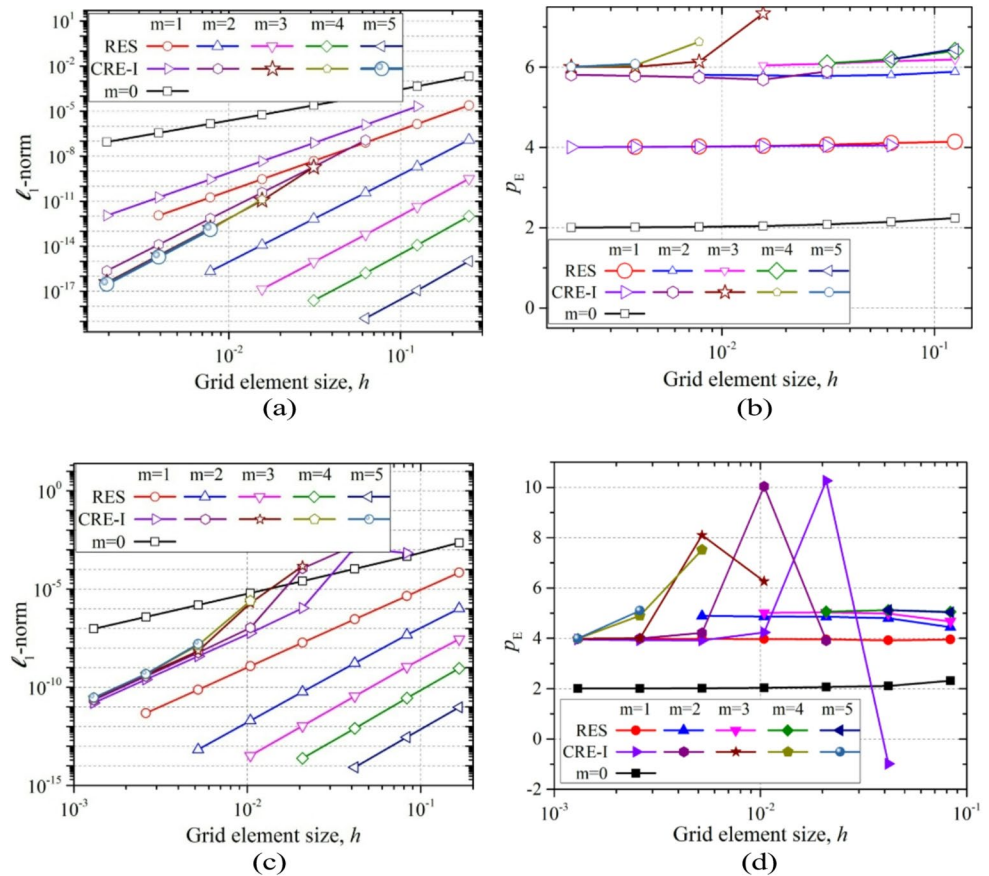
#### 4.1 2D Poisson equation

Simulations were performed for the 2D Poisson equation using initial grids with dimensions of  $5 \times 5$  and  $7 \times 5$ , which were uniform and non-uniform, respectively. Some results are presented in Fig. 11. The curves represent the  $\ell_1$ -norm of the discretization error and its corresponding effective order  $p_E$  as a functions of the grid size and the number of extrapolations, denoted by  $m$ . Each curve corresponds to an extrapolation level for a specific grid with spacing  $h$ . The curve associated with the numerical solution without extrapolation is indicated by  $m=0$ , whereas  $m=1$  represents one extrapolation, and so on.

Figure 11 presents the results of the RES and CRE-I methods applied to the 2D Poisson equation. Figure 11a and b show the results obtained with uniform grids.

As illustrated in Fig. 11a, the error is significantly reduced with  $m=1$  and  $m=2$ , and modestly with  $m=3$  for CRE-I. For  $m=4$  and  $m=5$ , identical results are obtained, indicating that further extrapolations have no additional effect. In the case of RES, the error is significantly reduced for all values of  $m$  from 1 to 5. Comparing the two methods, it is observed that, for the same values of  $h$  and  $m$ , RES exhibits a lower

**Fig. 11** 2D Poisson with RES and CRE-I: **a, b**  $5 \times 5$  initial uniform grid, **c, d**  $7 \times 5$  initial non-uniform by direction



error, making it more efficient than CRE-I in reducing the discretization error. In terms of order of accuracy, as shown in Fig. 11b, both methods yield the same results: for  $m=1$ , the order tends to 4, and for  $m=2$  or higher, it tends to 6.

That is, an increase of four orders of accuracy is achieved compared to the initial order of 2 for numerical solutions without extrapolation,  $m=0$ . Figure 11c and d show the results of simulations performed with non-uniform grids in each direction. As seen in Fig. 11c, for CRE-I, the error is significantly reduced only for  $m=1$ ; for  $m=2$  to  $m=5$ , the error increases compared to  $m=1$  for the same  $h$ , meaning that extrapolation worsens the numerical result. In the case of RES, the error is significantly reduced for all values of  $m$  from 1 to 5.

Comparing the two methods, it is observed that RES exhibits a lower error, for the same  $h$  value and any  $m$ , making it more efficient than CRE-I in reducing the discretization error. Regarding order of accuracy, as shown in Fig. 11d, CRE-I tends to 4 for any  $m \geq 1$ . In the case of the RES method, an order of 4 is obtained with  $m=1$ , and 5 for  $m \geq 2$ . Therefore, the CRE-I method achieves an increase of 2 orders of accuracy compared to the initial order of 2 for numerical solutions without extrapolation,  $m=0$ , whereas the RES method achieves an increase of 3 orders.

### 4.2 Nonlinear 1D Burgers equation

The simulations for the one-dimensional nonlinear model, Eq. (1) with  $Re=1$ , were performed with 11 points on the coarsest grid and refinement up to 163,841 points on the finest grid for both uniform and non-uniform cases. Each curve in Fig. 12 represents a level of extrapolation  $m$  as illustrated in Fig. 4 of Sect. 3.1. The oscillation in the determination of  $p_E$  when the number of extrapolations increases,  $m > 1$ , occurs when the numerical error is dominated by round-off errors, since the definition of  $p_E$ , Eq. (24), is valid for the discretization error [32]. From the third extrapolation onward, the curves were omitted for the CRE-I and FRE methods because the extrapolated solutions are coincident.

Figure 12a and b illustrate the results of applying the RES, CRE-I, and FRE methods on uniform grids. For  $m=1$ , the three methods show approximately the same error curve. However, for  $m \geq 2$ , the FRE method does not reduce the error compared to  $m=1$ ; on the other hand, the CRE-I and RES methods continue to reduce the error as  $m$  increases, with RES showing lower error for the same  $m$  and  $h$ . In terms of order of accuracy, as shown in Fig. 12b, the order of the FRE method is 4 for any  $m$ ; for the CRE-I and RES methods, an increase of 2 orders is obtained with each additional  $m$ , reaching order 12 for RES when  $m=5$ .

**Fig. 12** RES, CRE-I and FRE, nonlinear 1D Burgers equation,  $\ell_1$ -norm and effective order of the discretization error  $p_E$ : **a, b** uniform grid; **c, d** non-uniform grid

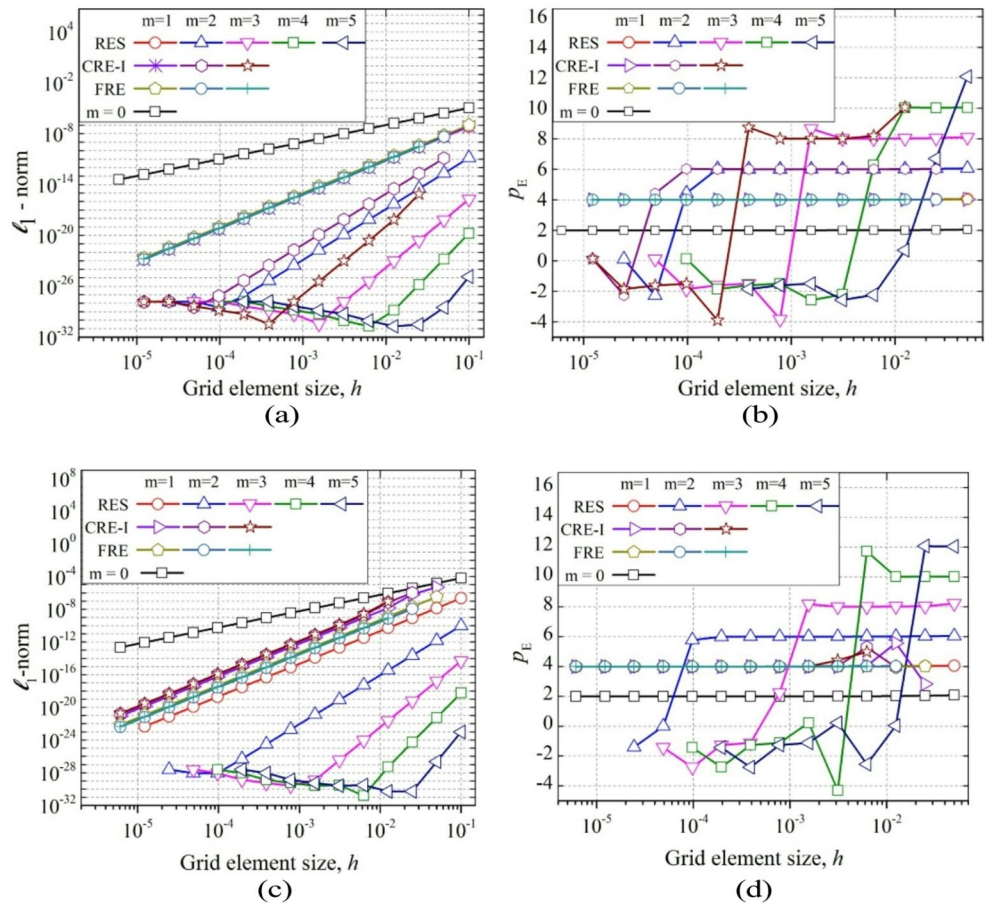


Figure 12c and d show the results of simulations performed with non-uniform grids. As seen in Fig. 12c, for FRE and CRE-I, the error is significantly reduced only for  $m=1$ ; for  $m=2$  and  $m=3$ , each method maintains the same error level as with  $m=1$  for the same  $h$ . In the case of RES, the error is significantly reduced for all values of  $m=1$  to 5. Comparing the three methods, it is observed that for the same value of  $h$  and any  $m$ , RES exhibits the lowest error, making it more efficient than CRE-I and FRE in reducing the discretization error. In terms of order of accuracy, as shown in Fig. 12d, FRE and CRE-I tend to 4 for any  $m \geq 1$ . In the case of the RES method, an order of 4 is obtained for  $m=1$ , with an increase of 2 orders for each additional  $m$ , reaching order 12 for RES when  $m=5$ ; this result is identical to the case with uniform grids.

Figure 13 presents some of the results obtained with the RRES method, as illustrated in the scheme in Fig. 5. In each curve, the first point on the right corresponds to the  $\ell_1$ -norm of the numerical solution for the chosen grid, without extrapolation, that is,  $m=0$ , while the second point on the same curve represents the  $\ell_1$ -norm of the numerical solution with  $m=1$ , and so on, until the lowest point on the curve, which represents the numerical solution with the

maximum number of extrapolations, according to the proposed approach.

For the grid  $g=14$ , which corresponds to 8192 points, only one extrapolation is performed because there is just one grid above it,  $g=15$ , which is the most refined grid with 16,384 points. It is observed that the RRES method uses a limited number of grids; however, the greater the availability of grids, the greater the opportunities to reduce the error, as evidenced in Fig. 13. Since the results follow the theoretical pattern of the RRE, as idealized in its construction, the effective order also shows significant growth, reaching  $p_E = 34$  at  $g=14$ , demonstrating the good performance of the method.

Table 2 shows the results of some simulations for RRES-I on three intermediate grids with 1281, 2561, and 5121 points. It was expected that RRES-I would yield results similar to RRES; however, for non-uniform grids, the values of the  $\ell_1$ -norm indicate that the discretization error affects the calculations of  $p_E$ , as in the previous case, resulting in values that cannot be considered. In the case of non-uniformity, where the  $\ell_1$ -norm on the finest grid reached a value of  $4.43 \times 10^{-15}$ , the effective order remained stable at  $p_E = 4$ , not following the same pattern as RRES.

**Fig. 13** RRES - SubGrid effect in nonlinear 1D Burgers equation on uniform grid

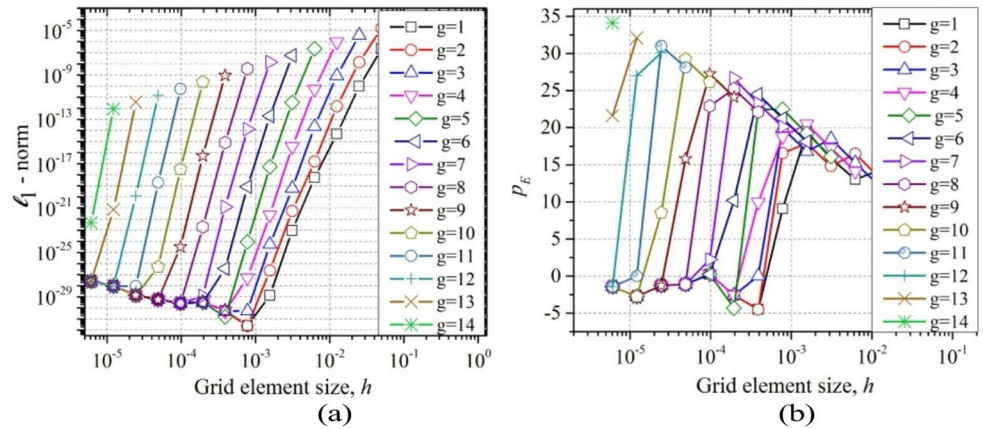


**Table 2** Results of RRES-I on intermediate grids for uniform and non-uniform cases

Grid	Uniform		Non-uniform	
	$\ell_1$ -norm	$p_E$	$\ell_1$ -norm	$p_E$
1281	1.38E-28	1.27E+01	1.1334E-12	4
2561	1.92E-31	9.49E+00	7.0882E-14	4
5121	8.40E-31	-2.13E+00	4.4319E-15	4

It is important to note that for both cases, the set of interpolated points  $\beta$  corresponds to the finest grid in the uniform case, with 16,384 points. Therefore, RRES-I, similar to the

previous case, showed inferior performance on non-uniform grids when compared to the other techniques used.

### 4.3 2D Burgers equations

In the 2D Burgers equations, Eqs. (13), uniform grids are considered, as shown in Fig. 1a of Sect. 2. The numerical solutions used to perform the extrapolations were obtained using the geometric multigrid method [5], which employs a hierarchy of grids, where the coarsest grid used was  $5 \times 5$ ,

**Fig. 14** 2D Burgers, RES and CRE-I,  $\ell_1$ -norm and effective order of the discretization error  $p_E$ : **a, b** velocity  $u$ ; **c, d** velocity  $v$

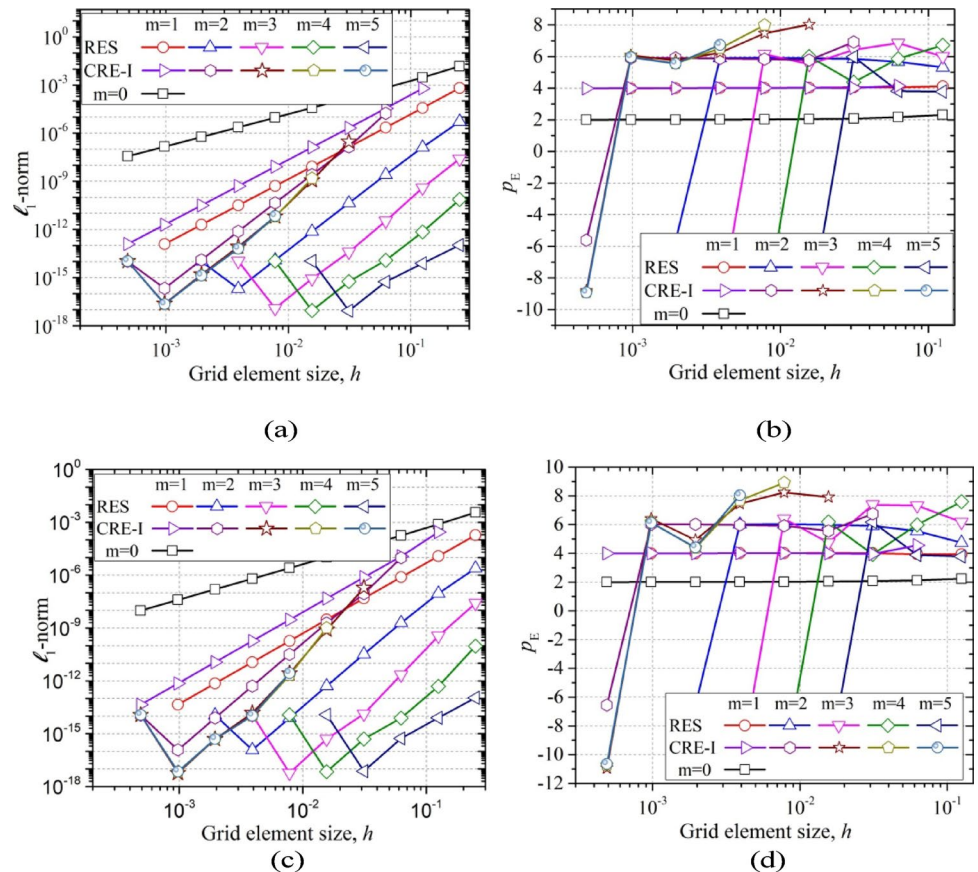
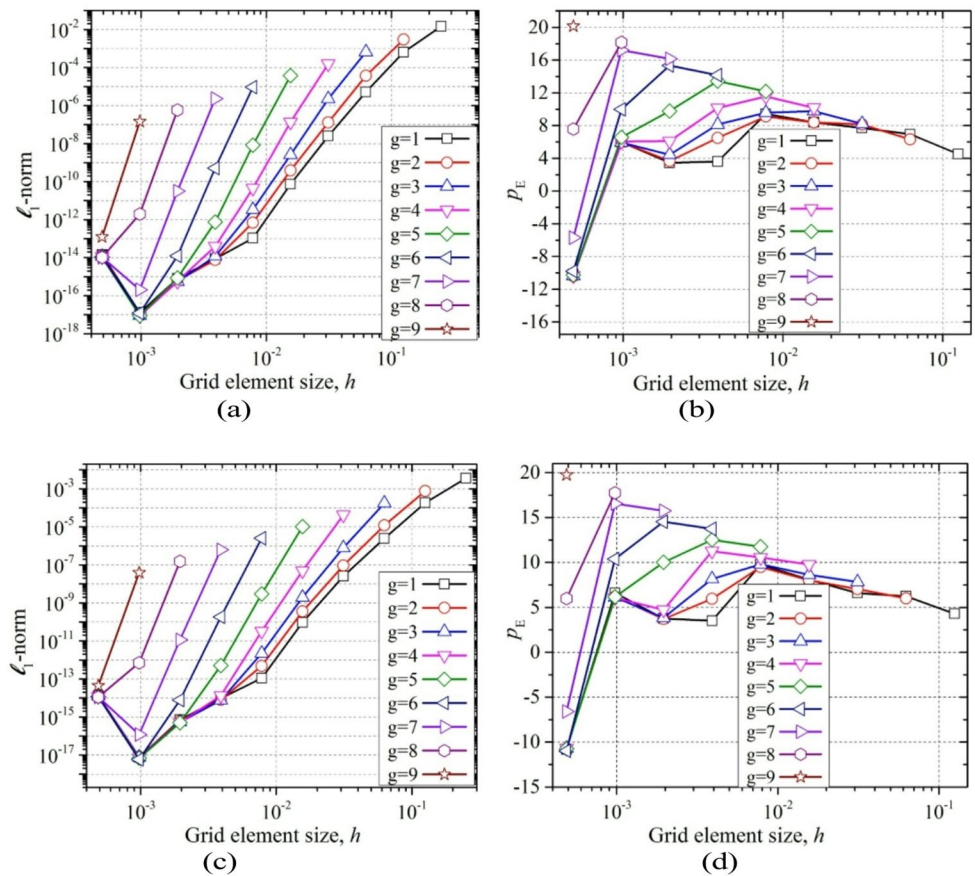


**Fig. 15** 2D Burgers equations on grids up to  $2049 \times 2049$  nodes with RRES: **a, c**  $\ell_1$ -norm reduction for  $u$  and  $v$ ; **b, d** effective order,  $p_E$ , of the discretization error for  $u$  and  $v$ , respectively



and the finest grid was  $2049 \times 2049$  points in each coordinate direction.

Figure 14 presents the results of the simulations for the  $\ell_1$ -norm and the effective order  $p_E$  of the  $\ell_1$ -norm, obtained with the RES and CRE-I methods for the velocities  $u$  and  $v$ . Each curve represents a level of extrapolation, where  $m=0$  is the non-extrapolated numerical solution. The abrupt reductions observed in the  $p_E$  curves and the inflections in the  $\ell_1$ -norm curves result from round-off errors in the numerical solutions, as the concept of  $p_E$  is valid for the discretization error.

As seen in Fig. 14a and c, for CRE-I, the error is significantly reduced only for  $m=1$  and  $m=2$ ; for  $m$  from 3 to 5, it remains at the same error level as for  $m=3$  for the same  $h$ . In the case of RES, the error is significantly reduced for all values of  $m$  from 1 to 5. Comparing the two methods, it is observed that for the same value of  $h$  and any  $m$ , RES exhibits lower error, making it more efficient than CRE-I in reducing the discretization error.

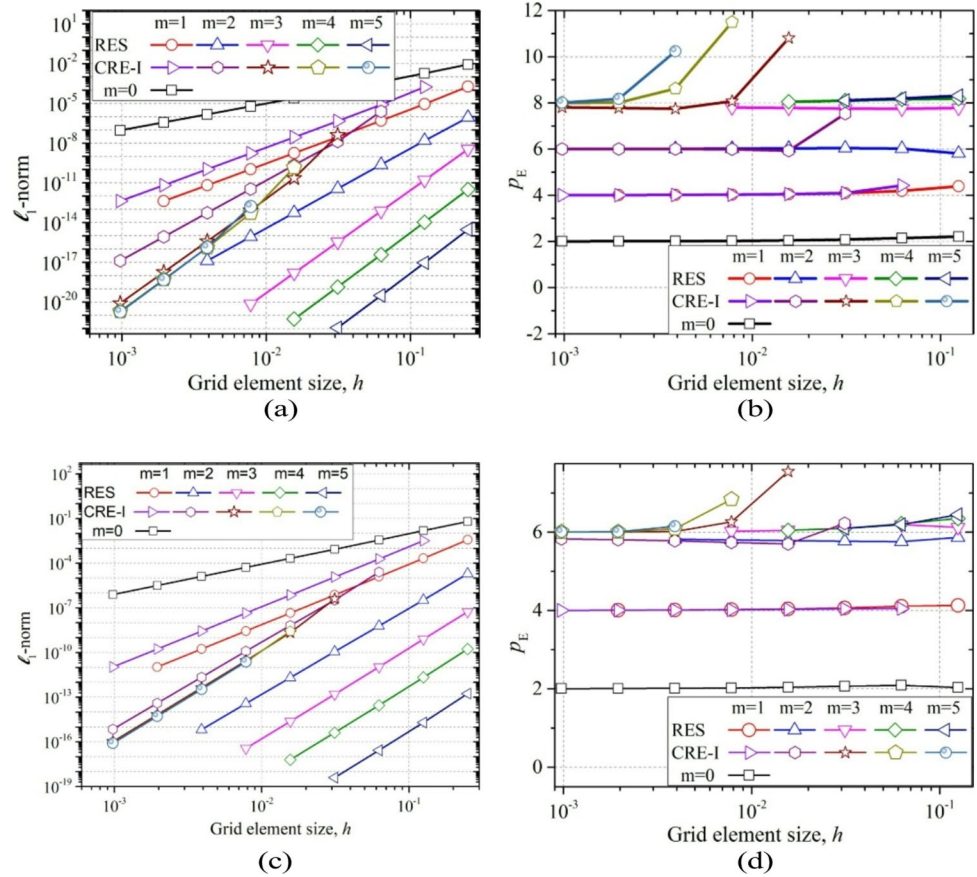
In terms of order of accuracy, as shown in Fig. 14b and d, both methods tend to 4 for  $m=1$  and to 6 for any  $m \geq 2$ . In [8],  $p_E = 4$  was found for the 2D Poisson equations, 1D advection-diffusion, 2D Laplace, and 2D Burgers in the velocity variable  $u$ .

Figure 15 presents the  $\ell_1$ -norm and  $p_E$  of the RRES method for the 2D Burgers equations in the velocities  $u$  and  $v$ , for 9 grids, as illustrated in the scheme shown in Fig. 5. In each curve, the first point on the right corresponds to the numerical solution for the chosen grid, without extrapolation,  $m=0$ , while the second point on the same curve represents the solution with  $m=1$ , and so on, until the lowest point on the curve, which indicates the maximum number of extrapolations, according to the proposed approach. For the grid  $g=9$ , corresponding to  $1025 \times 1025$  points, only one extrapolation is performed since there is only one finer grid available,  $g=10$ , which is the most refined grid with  $2049 \times 2049$  points. It is important to note that in the RRES method, the greater the number of available grids, the greater the opportunities for error reduction, as can be observed in Fig. 15a and c.

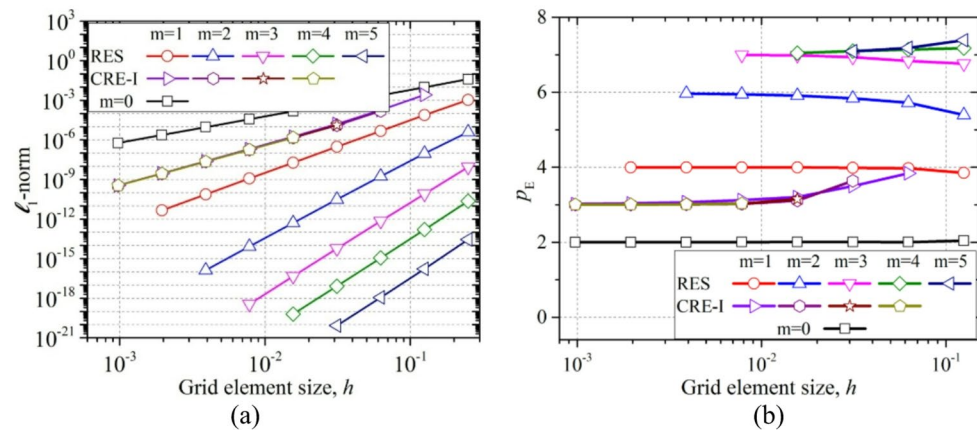
The results show a significant reduction in the  $\ell_1$ -norm, as well as an increase in the effective order,  $p_E$ , as seen in Fig. 15b and d, which correspond to the expected theoretical result when using the RRES method. It is also observed that the performance is superior on coarser grids, as well as  $p_E$  values that are affected by round-off errors.

For the velocity  $u$ , the  $\ell_1$ -norm was reduced to  $8.61 \times 10^{-18}$  at  $g=4$  and  $m=6$ . On grids  $g \leq 7$ , the calculations were

**Fig. 16** Navier-Stokes equations, RES and CRE-I: **a, b** streamfunction  $\psi$ , **c, d** vorticity  $\omega$



**Fig. 17** Navier-Stokes equations, CRE-I and RES, velocity  $u$ : **a**  $l_1$ -norm, **b**  $p_E$



affected by round-off errors. For the velocity  $v$ , similar qualitative results are observed. The increase in the effective order values with  $m$  demonstrates the excellent performance of the RRES method.

Compared to the results before applying any post-processing method, when  $p_0=2$ , it can be stated that the RRES method achieved an improvement of up to 9 orders on refined grids. It is observed that the  $p_E$  values increase with grid refinement. Therefore, in simulations with a greater availability of grids, it is expected that an even more significant

error reduction and an additional increase in order of accuracy will occur.

### 4.4 Navier-Stokes equations

The numerical solutions of the Navier–Stokes equations, Eq. (7), were obtained on uniform grids using the geometric multigrid method, with  $5 \times 5$  points on the coarsest grid and  $1025 \times 1025$  on the finest one. Figure 16 illustrates the results of the RES and CRE-I methods for the streamfunction  $\psi$  and vorticity  $\omega$  variables. Each curve represents an

**Table 3** Orders of accuracy,  $p_E$ , achieved by different methods for various equations

Equations	RES	CRE-I	RRES	RRES-I	FRE
2D Poisson					
Uniform	6	6			4
Non-Uniform	5	4			
1D Burgers					
Uniform	12	8	34	13	4
Non-Uniform	12	4	4	4	
2D Burgers	6	6	20		4
2D Navier-Stokes					
Streamfunction	8	8			
Vorticity	6	6			
Velocity	7	3			

extrapolation level for a given grid spacing  $h$ , where  $m=0$  indicates the numerical solution without extrapolation.

As seen in Fig. 16a and c, for CRE-I, the error is significantly reduced only for  $m$  from 1 to 3; for  $m=4$  and  $m=5$ , it remains at nearly the same level as for  $m=3$  at the same  $h$ . In the case of RES, the error is significantly reduced for all values of  $m$  from 1 to 5. Comparing the two methods, it is observed that, for the same  $h$  and any  $m$ , RES exhibits a lower error, making it more efficient than CRE-I in reducing discretization error.

In terms of order of accuracy, as shown in Fig. 16b, both methods tend to 4 and 6 for  $m=1$  and  $m=2$ , respectively, and to 8 for any  $m \geq 3$ . In the case of Fig. 16d, both methods tend to 4 for  $m=1$ , and to 6 for any  $m \geq 2$ .

Figures 17 present the  $\ell_1$ -norm and  $p_E$  curves obtained with the RES and CRE-I methods for the velocity  $u$  of the Navier–Stokes equations, Eq. (9). In Fig. 17a, it can be observed that the CRE-I method reduces the error only for  $m=1$ ; for  $m=2$  to 4, the error levels are equivalent to those of  $m=1$ . However, in the case of the RES method, the error decreases at each additional level of  $m$ , resulting in RES having a lower error than CRE-I for the same  $m$  and  $h$ .

In terms of order of accuracy, as shown in Fig. 17b, the CRE-I method maintains an order of 3 for any  $m$  ( $1 \leq m \leq 4$ ). In contrast, the RES method achieves orders of 4, 6, and 7 for  $m=1$  to 3, respectively, and for  $m=4$  and 5, the order remains at 7.

It is emphasized that  $u$  is approximated during post-processing and only on the finest grid of each V-cycle of the multigrid method during the iterative process. The results for the velocity  $v$  are qualitatively similar. Erturk et al. [7] achieved  $p_E = 6$  for the Navier–Stokes equations in the same formulation using the RRE method.

These behaviors can be explained by the numerical structure of the extrapolation methods. In RES, the extrapolated values from the finer grid replace the corresponding values on the coarser grid at coincident points, suppressing local truncation errors before they propagate through the domain.

In contrast, CRE-I requires interpolation at non-coincident nodes, which may introduce additional local errors, while FRE applies global corrections that do not preserve local consistency. Because these mechanisms operate solely on the discretization error structure, the qualitative behavior is similar for all tested models (Poisson, Burgers and Navier–Stokes), regardless of their physical characteristics.

## 5 Conclusion

In this article, the application of Richardson Extrapolation (RE) with SubGrid (RES), as well as methods such as CRE-I, RRES, and FRE, in numerical solutions of partial differential equations was investigated. The equations were discretized using the second-order accurate central difference scheme (CDS-2). Uniform, non-uniform, and directionally uniform grids were analyzed. The main objective was to improve the accuracy of numerical solutions, evaluated through the effective order of error measured using the  $\ell_1$ -norm. The expected accuracy,  $p_0=2$ , of numerical solutions without extrapolation ( $r_0$ ) was confirmed in all analyzed cases.

The conclusions presented here assume: (i) uniformly refined grids with a refinement ratio  $r=2$ , which ensures consistent comparison among grid levels; (ii) numerical solutions that exhibit regular convergence behavior, enabling the use of Richardson extrapolation; and (iii) that the extrapolation acts primarily on the discretization error structure, being largely independent of the physical nature of the governing equations.

The superior performance of the RES method compared to CRE-I and FRE is mainly associated with its local strategy for transferring extrapolated values between coincident nodes, which suppresses truncation errors before they propagate through the computational field. CRE-I relies on interpolation at non-coincident points, which may introduce additional numerical noise, while FRE applies global corrections that do not ensure local consistency. These differences explain the consistent advantage of RES across all analyzed models.

Table 3 summarizes the highest orders of accuracy obtained in this study with the grids, mathematical models, and methods used to reduce discretization error. It shows that the use of RE and RRE with SubGrid, i.e., the RES and RRES methods, is efficient in reducing discretization error across various types of problems, for both uniform and non-uniform grids. Moreover, these techniques are simple to implement and use.

Although all test cases in this study admit analytical solutions, the RES and RRES methods are also suitable for industrial CFD problems in which analytical solutions are

not available, such as turbulence, multiphase flows, and nonlinear transport phenomena. Recent studies involving complex multiphysics models, such as radiative magnetohydrodynamic nanofluid flows [3] and nonlinear reaction–diffusion systems [34], highlight scenarios where discretization errors significantly impact solution quality and where post-processing strategies like RES may offer substantial gains in accuracy. In the absence of a reference field, a promising direction is the combination of RES with numerical or machine-learning error estimators to guide the extrapolation process. Future developments will also explore extensions to three-dimensional unstructured grids, non-homogeneous boundary conditions, and the coupling of RES with higher-order finite volume or finite element formulations, aiming at improving accuracy in real-world CFD applications.

**Acknowledgements** The authors acknowledge the Department of Mechanical Engineering of Federal University of Paraná (UFPR), the Federal University of Technology - Paraná (UTFPR) in Apucarana, and the Conselho Nacional de Desenvolvimento Científico e Tecnológico (CNPq), Brazil, for the physical and financial support given for this work. This study was financed in part by the Coordenação de Aperfeiçoamento de Pessoal de Nível Superior (CAPES), Brazil, Finance Code 001. Cosmo D. Santiago and Carlos A. R. Carvalho, Jr. thank supported by CAPES scholarships. Carlos H. Marchi was supported by a CNPq scholarship.

**Author contributions** All authors contributed equally to this work.

**Funding** The Article Processing Charge (APC) for the publication of this research was funded by the Coordenação de Aperfeiçoamento de Pessoal de Nível Superior - Brasil (CAPES) (ROR identifier: 00x0ma614). This research was partially supported by Coordenação de Aperfeiçoamento de Pessoal de Nível Superior (CAPES). Not all authors received funding.

**Data availability** The data that has been used may be provided under reasonable request.

**Materials availability** Not applicable.

**Code availability** The code that has been used may be provided under reasonable request.

## Declarations

**Conflict of interest** The authors declare that they have no competing interests related to the content of this manuscript.

**Ethics approval and consent to participate** Not applicable.

**Consent for publication** Not applicable.

**Open Access** This article is licensed under a Creative Commons Attribution 4.0 International License, which permits use, sharing, adaptation, distribution and reproduction in any medium or format, as long as you give appropriate credit to the original author(s) and the source, provide a link to the Creative Commons licence, and indicate if changes were made. The images or other third party material in this

article are included in the article's Creative Commons licence, unless indicated otherwise in a credit line to the material. If material is not included in the article's Creative Commons licence and your intended use is not permitted by statutory regulation or exceeds the permitted use, you will need to obtain permission directly from the copyright holder. To view a copy of this licence, visit <http://creativecommons.org/licenses/by/4.0/>.

## References

- Richardson LF (1910) The approximate arithmetical solution by finite differences of physical problems involving differential equation, with an application to the stresses in a masonry dam. *Philos Trans R Soc Lond* 14(3):342–351. <https://doi.org/10.1098/rsta.1911.0009>
- Richardson LF (1927) J.A. <Gaunt The deferred approach to the limit. *Philosophical Proc Royal Soc Lond Serial A* 226 636–646 299–361 <https://doi.org/10.1098/rsta.1927.0008>
- Marchi CH, Novak LA, Santiago CD, Vargas APS (2013) Highly accurate numerical solutions with Repeated Richardson Extrapolation for 2D Laplace equation. *Appl Math Model* 37(12):7386–7397. <https://doi.org/10.1016/j.apm.2013.02.043>
- Dubeau F (2019) A remark on Richardson's Extrapolation process and numerical differentiation formulae. *J Comput Physics: X* 2:100017. <https://doi.org/10.1016/j.jcpx.2019.100017>
- Briggs WL, Henson VE, McCormick SF (2000) *A Multigrid Tutorial*, 2nd edn. Society for Industrial and Applied Mathematics, USA
- Benjamin AS, Denny VE (1979) On the convergence of numerical solutions for 2D flows in a cavity at large Re. *J Comput Phys* 33(3):340–358. [https://doi.org/10.1016/0021-9991\(79\)90160-8](https://doi.org/10.1016/0021-9991(79)90160-8)
- Erturk TCE, Corke, Gökçöl C (2005) Numerical solutions of 2D steady incompressible driven cavity flow at high Reynolds numbers. *Int J Numer Methods Fluids* 48:747–774. <https://doi.org/10.1002/fld.953>
- Marchi CH, Martins MA, Novak LA, Araki LK, Pinto MAV, Gonçalves SdFT, Moro DF, Freitas IdS (2016) Polynomial interpolation with Repeated Richardson Extrapolation to reduce discretization error in CFD. *Appl Math Model* 40:8872–8885. <https://doi.org/10.1016/j.apm.2016.05.029>
- Silva LP, Marchi CH, Meneguette M, Foltran AC (2022) Robust RRE technique for increasing the order of accuracy of SPH numerical solutions. *Math Comput Simul* 199:231–252. <https://doi.org/10.1016/j.matcom.2022.03.016>
- Roache PJ, Knupp PM (1993) Completed Richardson Extrapolation. *Commun Numer Methods Eng* 9:365–374. <https://doi.org/10.1002/cnm.1640090502>
- Silva NDP, Marchi CH, Araki LK, Borges RBdR, Bertoldo G, Shu C-W (2020) Completed Repeated Richardson Extrapolation for compressible fluid flows. *Appl Math Model* 77:724–737. <https://doi.org/10.1016/j.apm.2019.07.024>
- Marchi CH, Giacomini FF, Santiago CD (2016) Repeated Richardson Extrapolation to reduce the field discretization error in computational fluid dynamics. *Numer Heat Transf Part B: Fundamentals* 70:340–353. <https://doi.org/10.1080/10407790.2016.1215702>
- Joyce DC (1971) Survey of extrapolation process in numerical analysis. *SIAM Rev* 13(4):435–490. <https://doi.org/10.1137/1013064>
- Corless RM, Ilie S, Essex C (2009) The computational complexity of extrapolation methods. *Math Comput Sci* 2:557–566. <https://doi.org/10.1007/s11786-009-0053-x>
- Liu L-B, Yang X (2021) Convergence analysis of Richardson Extrapolation for a quasilinear singularly perturbed problem with

- an integral boundary condition on an adaptive grid. *Appl Math Lett* 115:106976. <https://doi.org/10.1016/j.aml.2021.106976>
16. da Silva LP, Pinto MAV, Araki LK (2024) Higher-order methods for the Poisson equation obtained with geometric multigrid and completed Richardson Extrapolation. *Comput Appl Math* 43(7):395. <https://doi.org/10.1007/s40314-024-02902-4>
  17. Fekete I et al (2025) Linear multistep methods with repeated global Richardson Extrapolation. arXiv preprint arXiv:2307.01345 (. <https://doi.org/10.1007/s10998-025-00654-0>
  18. Russo E (2024) Quantum error mitigation by layerwise Richardson Extrapolation. arXiv preprint arXiv:2402.04000 (. <https://doi.org/10.48550/arXiv.2402.04000>
  19. Street RL, Ferziger JH, Perić M (2020) Computational methods for fluid dynamics. Springer, Cham. <https://doi.org/10.1007/978-3-319-99693-6>
  20. Pletcher RH, Tannehill JC, Anderson DA (1997) Computational fluid mechanics and heat transfer
  21. Roache PJ (1998) Verification and validation in computational science and engineering. Hermosa publ., Albuquerque, USA
  22. Hwang BC, Shih TM, Tan CH (1989) Effects of grid staggering on numerical schemes. *Int J Numer Methods Fluids* 9:193–212. <https://doi.org/10.1002/flid.1650090203>
  23. Santiago CD, Marchi CH, Souza LF (2015) Performance of geometric multigrid method for coupled two-dimensional systems in CFD. *Appl Math Model* 39(9):2602–2616. <https://doi.org/10.1016/j.apm.2014.11.041>
  24. Anishchandran C, Manoharan A (2019) Performance optimization of tridiagonal matrix algorithm TDMA on multicore architectures: Computational framework and mathematical modelling. *Int J Grid High Perform Comput* 11:1–12. <https://doi.org/10.4018/IJGHPC.2019100101>
  25. Schneider GE, Zedan M (1981) A modified strongly implicit procedure for the numerical solution of field problems. *Numer Heat Transf* 4(1):1–19. <https://doi.org/10.1080/01495728108961724>
  26. Freundl C, Růžička U (2011) Gauss-Seidel iterative method for the computation of physical problems. In: Numerical mathematics and advanced applications, pp. 295–304. Springer, Berlin, Heidelberg. <https://doi.org/10.1007/978-3-642-14360-228>
  27. Osborne R (1883) An experimental investigation of the circumstances which determine whether the motion of water shall be direct or sinuous, and of the law of resistance in parallel channels. *Trans R Soc Lond* 174:935–982
  28. Roache PJ (2009) Fundamentals of verification and validation. Hermosa publ, Albuquerque, USA
  29. Roache PJ (1994) Perspective: a method for uniform reporting of grid refinement studies. *J Fluids Eng* 116:405–413. <https://doi.org/10.1115/1.2910291>
  30. Dai R, Zhang J, Wang Y (2013) Sixth order compact approximation with completed richardson extrapolation. In: International conference on computational and information sciences, pp. 966–971
  31. Zhang JR, Dai R, Wang Y (2016) Higher order ADI method with completed richardson extrapolation for solving unsteady convection-diffusion equations. *Comput Math Appl* 71:431–442. <https://doi.org/10.1016/j.camwa.2015.10.017>
  32. Marchi CH, Germer EM (2013) Effect of ten CFD numerical schemes on Repeated Richardson Extrapolation (RRE). *J Appl Comput Math* 2 <https://doi.org/10.4172/2168-9679.1000128>
  33. Ahmad H et al (2024) Entropy generation on MHD motion of hybrid nanofluid with porous medium in presence of thermo-radiation and ohmic viscous dissipation. *Discov Appl Sci* 6(4):199. <https://doi.org/10.1007/s42452-024-05866-6>
  34. Ahmad H et al. (2024) Numerical study of the reaction diffusion prey–predator model having holling ii increasing function in the predator under noisy environment. *J Nonlin Math Phys* 31(1):68 <https://doi.org/10.1007/s44198-024-00238-5>

**Publisher's note** Springer Nature remains neutral with regard to jurisdictional claims in published maps and institutional affiliations.